

Simulation based Analysis of FPGA Controlled Cascaded H-Bridge Multilevel Inverter Fed Solar PV System

KONE Ibrahima

Higher teacher training school of Bamako, (Ecole Normale Supérieure de Bamako)

Abstract: *In this paper we have studied the modeling of photovoltaic solar panels, the buck-boost converter and multi-level asymmetric H-bridge inverter. We have proposed a buck-boost converter control strategy and a multilevel inverter control strategy based on Nearest Level Modulation. The results of the simulation performed with the PSCAD-EMTDC software show that the proposed models and control strategies can be used in a photovoltaic system. This article can be considered as an update of the models used and a complement in the control of multilevel asymmetric H-bridge inverters.*

Keywords: photovoltaic solar panel, Buck-boost converter; Asymmetric Full bridge converter; nearest level modulation

1. Introduction

The cost of photovoltaic solar panels is becoming lower and lower in the world because of mastery of their manufacturing technology. In order to increase electricity coverage in our African countries, we must seek to lower the cost of isolated converters and even electric grid tied converters. The short-circuit current of a panel increases with illumination while the open-circuit voltage varies slightly. The open-circuit voltage and maximum power of a photovoltaic panel decrease very slightly when the temperature rises [4], [5]. In order to adapt the output voltage of the panels to the converter input voltage which is lower [9, 10, 11], in some works the buck converter controlled by the MPPT are used to control photovoltaic panel systems. Sometimes the boost converter controlled by the MPPT [14], [15] are used to adapt the output voltage of the panels to the converter input voltage which is higher.

We opted here for a buck-boost converter, because the variation range of the panel voltage is wide depending on the change in brightness and ambient temperature during the day, or one season to another. This converter will allow to adapt the output voltage of the panels to the input voltage of the converters in both directions [8].

The development of power electronics brings us a lot of solutions like the two levels converters, the three levels and even multilevel converters. The NPDC structure is presented by Nabae [16] and yuan [17]. The FC topology is presented by Meynard [18], the cascade structure of H bridge converter module is presented by Marchesoni [19] and Hammond [20]. Most of these different technologies often use transformers and filters to generate quasi-sinus voltages. To produce a pure sinus output voltage with very little harmonic content, thus limiting the size of the filters and even the transformers, we propose in this project the asymmetrical multilevel converter in bridge H. The cells of such a converter are powered by isolated voltage sources. Our isolated voltage sources consist of voltaic solar panels controlled by a buck-boost converter.

2. Photovoltaic Solar Panel Modeling

Generally the panel is modeled as a current generator.

Several electric models have been proposed to represent the photovoltaic cell whose model with a single diode [2], the model with two diodes [3]. In this project we propose the model with a single diode that will functions as a generator of current and voltage around its operating point as shown in figure 1.

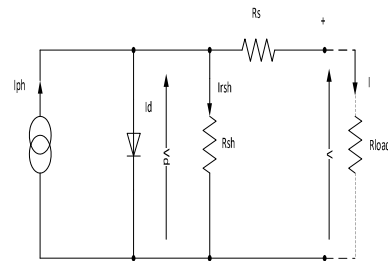


Figure 1: Model with a single diode

Where I_{ph} represents the photo current, R_s and R_{sh} respectively represent the series resistance and the parallel resistance of the photovoltaic cell.

The current flowing in the cell when the load connected to a receiver is given by the formula:

$$I = I_{ph} + I_d + I_{rsh} \quad (1)$$

Where, I_d the diode current and I_{rsh} the current in the parallel resistance.

The equation of the photo current as a function of solar irradiation and temperature is expressed in the De Soto model [1].

$$I_{ph} = I_{SCR} \frac{G}{G_{ref}} [1 + \alpha_T (T_{cell} - T_{cellref})] \quad (2)$$

The current of the diode is expressed by the equation:

$$I_d = I_0 \left(\exp \left(\frac{q \cdot V_d}{\gamma \cdot K \cdot T_{cell}} \right) - 1 \right) \quad (3)$$

Expressing the diode voltage according to the output parameters of the cell (I and V), we can write:

$$v_d = V + IR_s \quad (4)$$

$$I_d = I_0 \left(\exp \left(\frac{q(V+IR_s)}{\gamma.K.T_c} \right) - 1 \right) \quad (5)$$

The diode saturation current is expressed by the equation:

$$I_o = I_{oref} \left(\frac{T_{cell}}{T_{cellref}} \right)^3 \exp \left[\left(\frac{1}{T_{cellref}} - \frac{1}{T_{cell}} \right) \frac{q e_g}{\gamma K} \right] \quad (6)$$

Where I_{oref} is the reference diode saturation current, K is the Boltzmann constant, T_{cell} is the effective temperature of the cells (in Kelvin), $T_{cellref}$ is the reference temperature of the cells (in Kelvin), q the charge of the electron, and γ the quality factor of the junction.

A photovoltaic module is generally constituted by connecting N_s cells in series and N_p photovoltaic cells in parallel.

Then the module equivalent parameters can be written as:

$$I_{pheq} = N_p I_{ph} \quad (7)$$

$$I_{deq} = N_p I_d \quad (8)$$

$$R_{seq} = \frac{N_s}{N_p} R_s \quad (9)$$

$$R_{sheq} = \frac{N_s}{N_p} R_{sh} \quad (10)$$

$$I_{rsh} = N_p I_{rsh} \quad (11)$$

The photovoltaic module current can be expressed by the formula:

$$I_m = I_{pheq} + I_{deq} + I_{rsh} \quad (12)$$

The photovoltaic module voltage is defined by:

$$V_m = N_s V \quad (13)$$

3. Modeling of the buck-boost converter and its control strategy

This converter combines both a buck converter and a boost converter. It can be supplied by DC or AC input voltages. A buck converter produces an output voltage between zero and its input voltage, while a boost converter produces an output voltage greater than its input voltage.

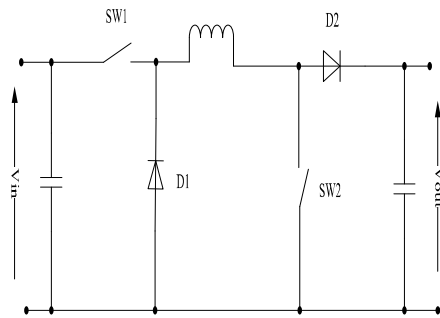


Figure 2: non-inverting buck boost converter

In continuous mode, when switching is done between 0 and DT : the switches $SW1$ and $SW2$ are ON and the diodes $D1$ and $D2$ are OFF.

$$\frac{dI_L}{dt} = \frac{V_{in}}{L} \quad (14)$$

$$\Delta I_{LON} = V_{in} \frac{DT}{L} \quad (15)$$

When switching is done between DT and T : the switches $SW1$ and $SW2$ are OFF and the diodes $D1$ and $D2$ are ON.

$$\frac{dI_L}{dt} = \frac{V_{out}}{L} \quad (16)$$

$$\Delta I_{LOFF} = V_{out} \frac{(T-DT)}{L} \quad (17)$$

Since the energy stored by the inductance at the beginning of the commutation is the same at the end of the commutation.

$$\frac{V_{out}}{V_{in}} = \frac{D}{1+D} \quad (18)$$

The duty cycle D of the non-inverting buck-boost converter can be expressed as follow:

$$D = \frac{V_{out}}{V_{out} + V_{in}} \quad (19)$$

According to the voltage V_{pv} and current I_{pv} of the solar photovoltaic panels, the MPPT [12], [13] controller generates the reference voltage V_{mppt} corresponding to the point of the photovoltaic generator maximum power. The difference between the voltage V_{mppt} and the voltage measured at the output of the buck-boost converter is controlled by a Proportional Integral PI regulator to give the duty cycle D .

To make this converter operate in booster mode, the switch $SW1$ is triggered ON and the PWM control signal is applied to the switch $SW2$. During this mode the capacitor $C2$ is charged by the sum of the input voltage and the voltage of the inductance L . The voltage of the capacitor $C2$ is transmitted to the output.

In order for this converter to operate in the step-down mode, the switch $SW2$ is triggered OFF and the PWM control signal is applied to the switch $SW1$. When the switch $SW1$ is blocked, the diode $D1$ conducts the current and ensures continuity of current flow at the output.

The duty cycle is compared with two triangular signals as shown in figure 5:

- If D is greater than $Saw2$, switch $SW2$ is ON and otherwise it is blocked;
- If D is greater than $Saw1$, switch $SW1$ is on and otherwise it is blocked.

When the duty cycle is less than 0.5, the converter operates as a step-down chopper while when the duty cycle is greater than 0.5, it operates as a booster chopper.

4. Modeling of the multilevel inverter and its control strategy

The proposed topology consists of series connection of H-bridge cells supplied by voltage sources of different values as in the references [21], [22]. In our project the solar photovoltaic panels controlled by buck-boost converter are used as voltage sources.

The DC input voltages for each cell are chosen according to a law which represents a geometric sequence of reason 3 and first term U_0 as follows:

$$V_{d_i} = U_0 3^{i-1} \quad \text{for } i = 1, 2 \dots p \quad (20)$$

Where i is the index of the cell in the converter, p the number of cells in the converter, U_0 is the unit input voltage of the cell.

This choice allows it to reduce the redundancy in the switching states of the converter switches and thus to have a high number of voltage levels in the inverter output voltage. Therefore, the output voltage of a cell can be expressed by:

$$Vsm_i = S_i \times Vd_i \quad (21)$$

Where S_i is the state of the cell as shown in Table 1.

The inverter output voltage can be expressed by the expression below:

$$Vout = \sum_{i=1}^p Vsm_i \quad (22)$$

The modulation techniques used to control multilevel converters in the literature compare triangular carriers with a reference as proposed in [23]. To mitigate or attenuate certain harmonics in the inverter output signal, paper [16] proposes calculating the switching angles.

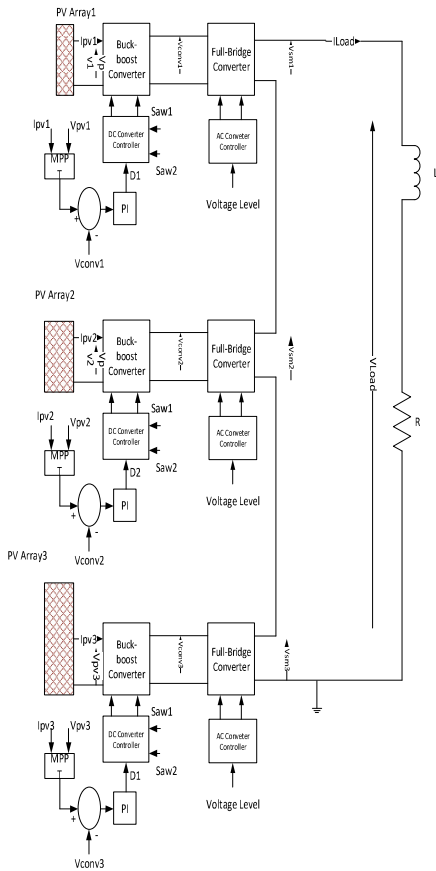


Figure 3: The proposed topology of 27 levels to asymmetrical H Bridge inverter driven by buck-boost converter

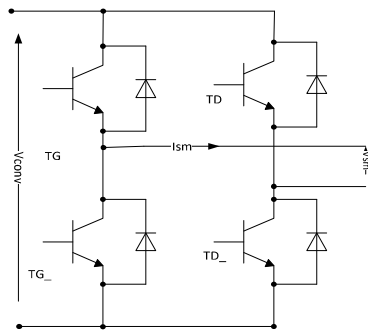


Figure 4: The H Bridge converter

Table 1: Switching states of an H-bridge module

Yes	TG	TD	Vsm	Ism
1	1	0	uo	iload
0	1	1	0	0
	0	0	0	0
-1	0	1	-Uo	-iload

Where TG are the Left switches and TD are the right switches. In a cell the states of the up and down switches are complementary

Table 2: The states of the modules of the inverter ($Vd1 = Uo$ $Vd2 = 3Uo$ $Vd3 = 9Uo$)

levels	Vsm1	VSM2	Vsm3	S1	S2	S3	vs.
27	uo	3Uo	9Uo	1	1	1	13Uo
26	0	3Uo	9Uo	0	1	1	12Uo
25	-Uo	3Uo	9Uo	-1	1	1	11Uo
24	uo	0	9Uo	1	0	1	10Uo
23	0	0	9Uo	0	0	1	9Uo
22	-Uo	0	9Uo	-1	0	1	8Uo
21	uo	-3Uo	9Uo	1	-1	1	7Uo
20	0	-3Uo	9Uo	0	-1	1	6Uo
19	-Uo	-3Uo	9Uo	-1	-1	1	5Uo
18	uo	3Uo	0	1	1	0	4Uo
17	0	3Uo	0	0	1	0	3Uo
16	-Uo	3Uo	0	-1	1	0	2uo
15	uo	0	0	1	0	0	uo
14	0	0	0	0	0	0	0
13	-Uo	0	0	-1	0	0	-Uo
12	uo	-3Uo	0	1	-1	0	-2Uo
11	0	-3Uo	0	0	-1	0	-3Uo
10	-Uo	-3Uo	0	-1	-1	0	-4Uo
9	uo	3Uo	-9Uo	1	1	-1	-5Uo
8	0	3Uo	-9Uo	0	1	-1	-6Uo
7	-Uo	3Uo	-9Uo	-1	1	-1	-7Uo
6	uo	0	-9Uo	1	0	-1	-8Uo
5	0	0	-9Uo	0	0	-1	-9Uo
4	-Uo	0	-9Uo	-1	0	-1	-10Uo
3	uo	-3Uo	-9Uo	1	-1	-1	-11Uo
2	0	-3Uo	-9Uo	0	-1	-1	-12Uo
1	-Uo	-3Uo	-9Uo	-1	-1	-1	-13Uo

To determine the voltage level, the difference between the maximum voltage and the reference voltage is divided by the unit voltage Uo for a first time before being digitized to the nearest whole number. The switching signals of the switches are generated from the voltage level as in Table 2. The reference voltage is determined as follows:

$$V_{ref} = mV_{max} \sin(\omega t + \phi) \quad (23)$$

Voltage levels can be calculated by the following equation:

$$level = INT\left(\frac{V_{max} - V_{ref}}{U_o}\right) \quad (24)$$

signals to transistors

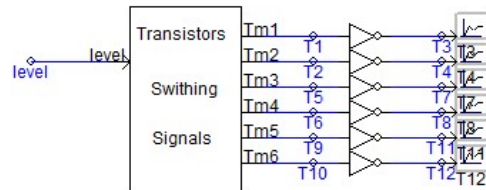


Figure 5: Switching Signals

5. The Simulation results

To verify the models and control strategies a simulation is performed in the PSCAD-EMTDC software with the parameters shown in the appendix. The output voltages of the three buck-boost converters are shown in Figure 6. These curves shows that the solar panels voltages applied to the converters inputs are adapted to the H-bridges inputs.

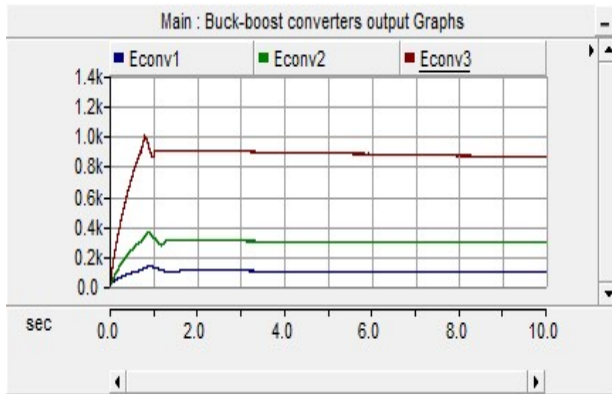


Figure 6: The shape of the voltages at the output of the buck-boost converters 1, 2 and 3

The curves of voltage levels detection and the control signals of each switch of the inverter at any instant are shown in figure 7.

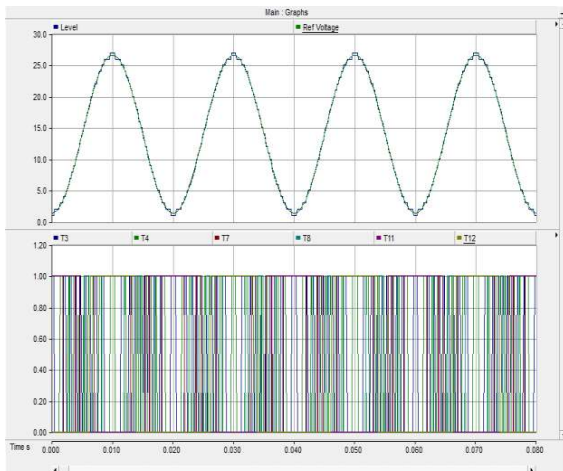


Figure 7: The curves of the voltage levels and the signals generated for the switches

The output voltage chronographs for each module (3 modules in this project) are shown in Figure 8. This figure shows that the cell from above produces the voltage level of 100 V, 0V and -100 V between its outputs, the middle cell produces the voltage level of 300 v, 0V and -300 V between its terminals and the cell of at the bottom produces the voltages level of 900 V, 0 V and -900 V between its terminals.

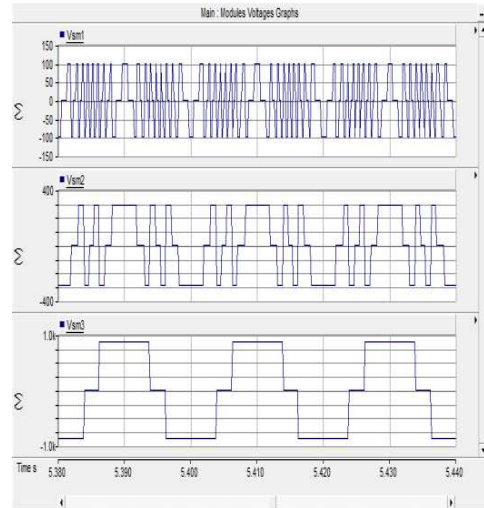


Figure 8: The curves of the output voltages of each H-bridge module

The curves of the voltage across the load and the current through the load are shown in Figure 9. As shown in this, the voltage and the current intensity are sinusoidal signals.

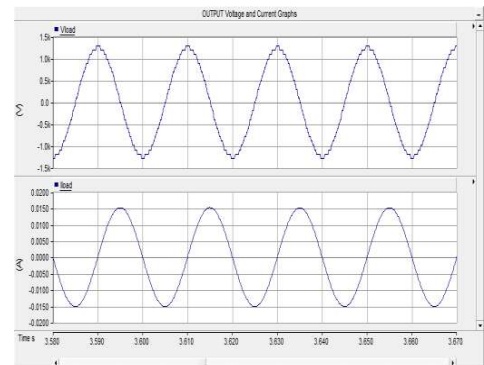


Figure 9: The chronographs of the voltage across the load and the current flowing into the load

6. conclusions

Based on the results of the simulation, the curves show that the converter gives voltages and currents close to the sinus, which results in the decrease in the size of the output filters and the need for a transformer. The multi-level topology control technique applied here reduces the frequency of switching power electronics switches. Such a device will be interesting as a photovoltaic system inverter. Such a device will be interesting for islanding photovoltaic systems even for grid-tied photovoltaic systems.

Appendix

<i>Buck-boost converter 1 parameters</i>	
Capacitor C1	9 000uF
Capacitor C2	90 000uF
Inductance L	0.001 1 H
The voltage of installed solar panels Vpv1	100V
<i>Buck-boostconverter 2 parameters</i>	
Capacitor C1	3 000uF
Capacitor C2	30 000uF
Inductance L	0.00 33 H
Voltage of installed solar panels Vpv2	300V
<i>Buck-boostconverter 3 parameters</i>	
Capacitor C1	1000uF

Capacitor C2	10 000uF
Inductance L	0.0 1 H
The voltage of installed solar panels Vpv3	900V
<i>Multi-level converter Control parameters</i>	
System frequency	50 Hz
Modulation index m	0.95
<i>Load parameters</i>	
R	5 0 Ω
The	261.31 mH
<i>Buck-boost converter Control parameters</i>	
Control frequency	2000 Hz
Saw1 amplitude	0.5
Saw2 amplitude	1.0

References

- [1] De Soto, W., Klein SA, et al. (2006). "Improvement and validation of a model for photovoltaic array performance." *Solar Energy* 80 (1): pp. 78-88.
- [2] Gray, JL., Luque A., Hegedus, S. The Physics of the Solar Cell, in *Handbook of Photovoltaic Science and Engineering*, Editor. 2011, John Wiley and Sons.
- [3] Ishaque, K., Salam, Z., and Taheri, H.: 'Accurate MATLAB Simulink PV system simulator based on a two-diode model', *Journal of Power Electronics*, 2011, 11, (2), pp. 179-187.
- [4] Priyanka Singh, "Solar Thermal Materials Materials and Solar Cells," "Temperature dependence of I-V characteristics and performance parameters of silicon solar cell." 92, no. 12, pp. 1611-1616, 2008.
- [5] Priyanka Singh, NM Ravindra, "Solar Energy Materi als and Solar Cells, Vol. 101, pp. 36-45, 2012.
- [6] Shengyi Liu and Roger A. Dougal, Dynamic Multiphysics Model for Solar Array, *IEEE Transactions on Energy Conversion*, Vol. 17 (2), June 2002.
- [7] AD Rajapakse, and D. Muthumuni, Simulation Tools for Photovoltaic Systems Grid Integration Studies, *Electrical Power and Energy Conference (EPEC)*, Montreal, Canada, October 22-23, 2009.
- [8] Chen J, Maksimovic D, R Erickson. "Buck-boost PWM converters having two independently controlled switches". *Power Electronics Specialists Conference, 2001. PESC. 2001.* 2001; 2, pp. 736-741.
- [9] A. Wiesner, R. Diez, and G. Perilla, "Design and Implementation of a Buck Converter with MPPT for Battery Charge from Solar Module," 2013 Workshop on Power Electronics and Power Quality Applications (PEPQA), Bogota, 2013, pp. 1-6.
- [10] U. KAMNARN, S. YOUSAWAT, S. SREETA, W. MUANGJAI and T. SOMSAK, "Design and Implementation of a Distributed Solar Controller Using Modular Buck Converter with Maximum Power Point Tracking," *IEEE*, 2009.
- [11] D. Lu, S. Sathiakumar, RH Chu and VG Agelidis, "A Buck Converter with Simple Maximum Power Point Tracking for Power Electronics Education on Solar Energy Systems," *IEEE*, 2007.
- [12] Yafaoui. A., Wu B. and Cheung R., Implementation of Maximum Power Point Tracking Algorithm for Residential Photovoltaic Systems, 2nd Canadian Solar Buildings Conference, Calgary, June 10 - 14, 2007.
- [13] Hussein KH, Muta I., Hoshino T., Osakada, M., Maximum photovoltaic power tracking: an algorithm for rapidly changing atmospheric conditions. *Generation, Transmission and Distribution, IEE Proceedings-Volume 142 Issue 1, Jan. 1995*, pp. 59 - 64.
- [14] Arun Kumar Verma, Bhim Singh and SC Kaushik, "An Isolated Solar Power Generation Using Boost Converter and Boost Inverter," in *Proc. National Conference on Recent Advances in Computational Technique in Electrical Engineering*, SLITE, Longowal, India, 19-20 March, 2010, paper 3011, pp.1-8.
- [15] Athimulam Kalirasu, Subharensu Sekar Dash, "The Simulation of Closed Loop Controlled Boost Converter for Solar Installation", *Serbian Journal of Electrical Engineering* Vol.7, No.1, May 2010, pp. 121-130.
- [16] A. Nabae and H. Akagi. A new neutral-point-clamped PWM inverter. *IEEE Transactions on Industry Applications*, 17 (5), pp.518-523, September 1981.
- [17] X. Yuan, L. Barbi: Fundamental of New Diode Clamping Multilevel Inverter. *IEEE Transactions on Power Electronics*, Vol.15, No 4, July 2000.
- [18] T. Meynard, H. Foch: Imbricated Cells Multilevel Voltage-Source Inverters for High-Voltage Applications. *EPÉE Journal*, vol.3 Jun 1993.
- [19] M. Marchesoni, M. Mazuchelli, S. Tenconi: A Non-Conventional Power Converter for Plasma Stabilization. *PESC 88*, 11-14 April 1988, Conf.Rec.Vol.2, pp. 626-633.
- [20] P. Hammond: A New Approach to Enhance Power Quality for Medium Voltage Drives. *IEEE Petroleum and Chemical Ind. conf.App*, pp. 231-235, September 1995.
- [21] MD Manjrekar and TA Lipo. A hybrid multilevel inverter topology for drive applications. *IEEE-APEC'98*, p. 523-529.
- [22] A. Rufer, M. Veenstra, and K. Gopakumar. Asymmetric multilevel converter for high resolution voltage phasor generation. *EPE'99*.
- [23] G. Carrara et al. A new multilevel PWM method: a theoretical analysis. *IEEE Transactions on Power Electronics*, 7 (3), pp.497-505, July 1992.